SPECIAL TOPIC — Phononics and phonon engineering

Ultra-low thermal conductivity of roughened silicon nanowires: Role of phonon–surface bond order imperfection scattering*

Heng-Yu Yang(杨恒玉)[1,2], Ya-Li Chen(陈亚利)[3], Wu-Xing Zhou(周五星)[1,2], Guo-Feng Xie(谢国锋)[1,2,†], and Ning Xu(徐宁)[4,2,‡]

[1] School of Materials Science and Engineering, Hunan University of Science and Technology, Xiangtan 411201, China
[2] Hunan Provincial Key Laboratory of Advanced Materials for New Energy Storage and Conversion, Xiangtan 411201, China
[3] School of Physics and Optoelectronics, Xiangtan University, Xiangtan 411105, China
[4] Deparment of Physics, Yancheng Institute of Technology, Yancheng 224051, China

(Received 31 March 2020; revised manuscript received 4 June 2020; accepted manuscript online 5 June 2020)

The ultra-low thermal conductivity of roughened silicon nanowires (SiNWs) can not be explained by the classical phonon–surface scattering mechanism. Although there have been several efforts at developing theories of phonon–surface scattering to interpret it, but the underlying reason is still debatable. We consider that the bond order loss and correlative bond hardening on the surface of roughened SiNWs will deeply influence the thermal transport because of their ultra-high surface-to-volume ratio. By combining this mechanism with the phonon Boltzmann transport equation, we explicate that the suppression of high-frequency phonons results in the obvious reduction of thermal conductivity of roughened SiNWs. Moreover, we verify that the roughness amplitude has more remarkable influence on thermal conductivity of SiNWs than the roughness correlation length, and the surface-to-volume ratio is a nearly universal gauge for thermal conductivity of roughened SiNWs.

Keywords: thermal conductivity, silicon nanowires, bond order imperfections, phonon–surface scattering

PACS: 65.80.–g, 63.22.–m **DOI:** 10.1088/1674-1056/ab99af

1. Introduction

Understanding and tuning the thermal transport in nanostructures are very important for the development of thermoelectric devices[1–11] and the thermal management of micro- and nano-electronics devices.[12–24] Because of the high surface-to-volume ratio (SVR) of nanostructures, the phonon–surface scattering results in the prominent size effect limiting the thermal transport. However the precise effects of surface on thermal transport have remained unclear because the mechanism of phonon–surface scattering is still not well understood. In many literatures, the effect of phonon-boundary scattering has been treated by assuming a constant value p,[25–28] which is a fitting parameter to simulate the probability of specular scattering. Ziman's formula[29] $p = \exp\left(-16\pi^2\delta^2/\lambda^2\right)$ is an improvement over the constant p model as it accounts for wavelength and surface roughness dependent scattering.[30–32] The thermal conductivities of silicon nanowires (SiNWs) calculated by Ziman's theory[33,34] agree well with the measurement results of comparatively smooth SiNWs grown by the vapor-liquid-solid (VLS) method.[35] However, the measured thermal conductivities of rough SiNWs obtained by electrochemical etching (EE) are much lower than the Casimir limit corresponding to complete momentum randomization at the surface ($p = 0$).[36] Ziman's theory fails to predict it, because further increase of surface roughness does not lead to appreciable reduction of thermal conductivity (κ) calculated by Ziman's theory. Several efforts have been made toward an accurate understanding of phonon surface scattering. Moore *et al.* predicted stronger backscattering of phonons at periodically rough surfaces by phonon Monte Carlo (MC) simulations.[37] Based on the Born approximation, Martin *et al.* used a perturbative approach to get the roughness scattering mechanism.[38] Sadhu and Sinha, using a wave-like phonon transport approach, considered coherent scattering of phonons from a rough surface.[39] Although these theoretical studies accounted for the surprisingly suppression of SiNWs by very rough surfaces, they could not well explain the experimental work by Lim *et al.*, which performed a systematic experimental study of the surface condition of intentionally roughened VLS-grown SiNWs and provided the first evidence for frequency-dependent phonon scattering from the rough surfaces.[40] By introducing the Beckmann–Kirchhoff based surface scattering theory, Malhotra and Maldovan calculated the wavelength heat spectrum and found that increased phonon surface scattering led to the shifts towards short phonon wavelengths and mean free paths.[41] However, by combining the Landauer model and spectral scaling model,

*Project supported by the National Natural Science Foundation of China (Grant No. 11874145).
†Corresponding author. E-mail: gfxie@xtu.edu.cn
‡Corresponding author. E-mail: nxu@ycit.cn

Lee *et al.* revealed that the experimentally measured ballistic phonon transport in the holey silicon with small neck size (only 20 nm) stemmed form filtering high-frequency phonons and increasing contribution of low-frequency phonons by surface scattering.[42] These contradictions imply that the mechanism of phonon–surface scattering in nanostructures requires further exploration.

The traditional phonon–surface scattering mechanism only takes into account the geometric constraints of the surface resulting in the change of motion of particles or waves, which is the numerical boundary attribute of the surface. The surface of a nanostructure terminates the periodicity of the lattice, but it is not simply equal to the mathematical boundary. The physical attributes of atoms near the surface are different from those in the bulk, for example, the atoms in the surface skin are under-coordinated. The loss of bond order makes the bonds of the under-coordinated atoms become shorter and stronger.[43,44] The bond shortening and strengthening in the surface skin provide a perturbation to the Hamiltonian of the lattice vibration system, and this under-coordination effect should play an important role in the phonon transport of nanostructures because of the ultra-high surface-to-volume ratio of the nanostructures. However, in the traditional models of phonon–surface scattering, this coordination dependent mechanism is overlooked. Very recently, base on the bond order theory and quantum perturbation theory, we presented a novel phonon–surface scattering mechanism from the perspective of bond order loss.[45] In this work, we combine this mechanism with the phonon Boltzmann transport equation (BTE). The calculation results agree well with the ultra low κ of intentionally roughened VLS SiNWs in experiments. It is revealed that the surface bond order imperfections play the dominant role in hindering transport of high-frequency phonons, which results in the obvious reduction of κ. Furthermore, we numerically generate the random roughness profile of SiNWs according to the given autocorrelation function, and detailedly analyze the effect of the geometrical parameters on κ of the roughened SiNWs.

2. Methods

On the basis of phonon BTE, the κ of phonons of the λ-th branch in the direction of $\nabla T(x)$ of the nanowire is derived as[46]

$$\kappa_\lambda = \frac{V}{(2\pi)^3}\int c_{\rm ph} v_x^2 \tau \mathrm{d}\boldsymbol{q}, \tag{1}$$

where V is the volume of the nanowire, v_x is the x component of the group-velocity, τ is the relaxation time, $\boldsymbol{q}$ is the wave vector, and $c_{\rm ph}$ is the volumetric specific heat of each mode. The κ of bulk and nanostructured silicon is often successfully modeled with an assumed isotropic dispersion.[30,47] Using the isotropic dispersions approximation, we can transform Eq. (1) from the integral of wave vector q to angular frequency ω, and get

$$\kappa_\lambda = \frac{1}{6\pi^2}\int_0^{\omega_{\rm m}} \frac{\hbar^2\omega^2}{k_{\rm B}T^2}\frac{\mathrm{e}^{\hbar\omega/k_{\rm B}T}}{\left(\mathrm{e}^{\hbar\omega/k_{\rm B}T}-1\right)^2} v(\omega)\tau(\omega)q^2(\omega)\mathrm{d}\omega, \tag{2}$$

where $\omega_{\rm m}$ is the Brillouin zone-boundary frequency of branch λ.

Based on phonon BTE, the κ of SiNWs can be calculated as $\kappa = \kappa_{\rm LA} + 2\kappa_{\rm TA}$. In order to calculate $\kappa_{\rm LA}$ and $\kappa_{\rm TA}$ by Eq. (2), the phonon wave vector and group velocity as a function of angular frequency must be determined by the phonon dispersions. Both first-principles calculations[48] and experimental measurements[49] indicate that the acoustic phonon dispersions in silicon are not linear. We adopt the quadratic approximation dispersion like that in Ref. [48], which is given by

$$\omega(q) = v_{\rm s}q + cq^2, \tag{3}$$

therefore $q(\omega)$ and $v(\omega)$ needed in Eq. (2) are derived as

$$q(\omega) = \frac{-v_{\rm s}+\sqrt{v_{\rm s}^2+4c\omega}}{2c} = \frac{v(\omega)-v_{\rm s}}{2c}, \tag{4}$$

$$v(\omega) = \frac{\mathrm{d}\omega}{\mathrm{d}q} = v_{\rm s}+2cq = \sqrt{v_{\rm s}^2+4c\omega}. \tag{5}$$

According to the Matthiessen's rule, the total phonon scattering rate in SiNWs is given as $\tau^{-1} = \tau_{\rm U}^{-1}+\tau_{\rm B}^{-1}+\tau_{\rm I}^{-1}+\tau_{\rm Bond}^{-1}$. Slack and Galginaitis suggested the umklapp phonon–phonon scattering rate as $\tau_{\rm U}^{-1}(\omega) = B_{\rm U}\omega^2 T\mathrm{e}^{-\Theta/3T}$, where $\Theta = \hbar\omega_{\rm m}/k_{\rm B}$ is the Debye temperature, which is calculated by Brillouin zone-boundary frequency $\omega_{\rm m}$.[50] The traditional diffusive phonon-boundary scattering rate is given by $\tau_{\rm B}^{-1} = v/D$, where D is the diameter of SiNWs. The phonon–impurity scattering rate is given by $\tau_{\rm I}^{-1}(\omega) = A\omega^4$, parameter $A = 1.32\times10^{-45}$ s^3 for natural silicon is analytically determined from the isotope concentration, and it should not be adjusted.[51] For silicon, derived from the quantum perturbation theory and the bond order theory in our recent work, the phonon–surface bond order imperfection scattering rate $\tau_{\rm Bond}^{-1}$ is given as[45]

$$\tau_{\rm Bond}^{-1} = 1.86\times10^{-51}\cdot{\rm SVR}\cdot\omega^4, \tag{6}$$

where SVR is the surface-to-volume ratio in units of m^{-1}. All the parameters mentioned above are listed in Table 1.

Table 1. Parameters in calculation of thermal conductivity of SiNWs.

Branch	$v_{\rm s}$/(m/s)	c/(10^{-7} m^2/s)	$\omega_{\rm m}$/(Trad/s)	Θ/K	$B_{\rm U}$/(10^{-19} s/K)
LA	9010	−2.0	77.5	592	0.908
TA	5230	−2.26	30.3	231	2.0

The SVR of nanowires in Eq. (6) is related with the geometric size, cross sectional shape, and surface roughness profile. Due to the isotropic nature of the etching process, we consider long SiNWs with circular cross-section and rough surfaces characterized by a given autocorrelation function (ACF),

as shown in Fig. 1. The SVR of SiNWs can be calculated by

$$\mathrm{SVR} = \frac{4\int_0^L 2\pi y(x)\sqrt{1+y'(x)^2}\mathrm{d}x}{\pi D^2 L}. \tag{7}$$

Here D and L are the diameter and length of the SiNWs, respectively, and $y(x)$ is the random roughness profile.

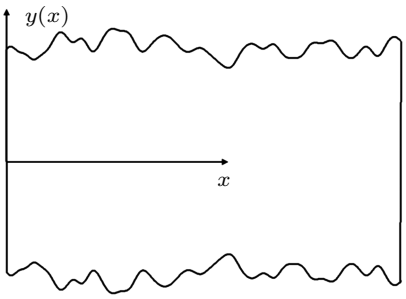

Fig. 1. Schematic illustration of surface roughness profile of SiNWs, where x is the longitudinal axis of the nanowires.

In order to calculate the SVR of the roughened SiNWs by Eq. (7) and investigate the effect of correlated surface roughness on thermal conductivity of SiNWs, we need to numerically generate the roughness profile $y(x)$ on the basis of ACF. It is generally assumed that the ACF of rough surface obeys the exponential curve or Gaussian curve,[52] which is given by

$$C(x) = \begin{cases} \delta^2 \mathrm{e}^{-x/\xi}, & \text{exponential}, \\ \delta^2 \mathrm{e}^{-x^2/\xi^2}, & \text{Gaussian}, \end{cases} \tag{8}$$

where ξ is the correlation length of roughness, and δ is the root-mean-square (rms) of roughness.

By the convolution theorem, the power spectrum density $S(q)$ is the Fourier transform of the ACF given by

$$S(q) = F[C(x)] = \begin{cases} \frac{2\delta^2\xi}{1+q^2\xi^2}, & \text{exponential}, \\ \frac{\sqrt{\pi}\delta^2\xi}{\mathrm{e}^{q^2\xi^2/4}}, & \text{Gaussian}, \end{cases} \tag{9}$$

where F stands for the Fourier transform. By the Wiener–Khinchin theorem,

$$|Y(q)|^2 = F[LC(x)] = LS(q), \tag{10}$$

where L is the length of the nanowire, and $Y(q) = F[y(x)]$ is the Fourier transform of surface roughness profile $y(x)$. Therefore we can generate the surface roughness profile $y(x)$ by one-dimensional inverse Fourier transform, which is given as[53]

$$y(x) = F^{-1}\left[|y(q)|\mathrm{e}^{\mathrm{i}\varphi_q}\right] = F^{-1}\left[\sqrt{LS(q)}\mathrm{e}^{\mathrm{i}\varphi_q}\right], \tag{11}$$

where F^{-1} stands for the inverse Fourier transform, and $\mathrm{e}^{\mathrm{i}\varphi_q}$ is an odd random phase for the spatial frequency of roughness q.

3. Results and discussion

Figure 2 compares the thermal conductivities computed from our above model vs. the experimental data from Ref. [40]. Herein the surface roughness profiles are obtained according to the exponential ACF, because the roughness parameters δ and ξ of the intentionally roughened SiNWs are extracted from exponential fits to the experimentally obtained ACFs in Ref. [40]. The parameters D, δ, and ξ are kept the same as those in Ref. [40]. Our model not only agrees well with the κ of smooth SiNW grown by VLS mechanism, but also reproduces the drastic decrease in the κ of the intentionally roughened SiNWs. In Fig. 2, the smooth SiNW (black line) and roughened SiNW (blue line) have nearly the same diameter, but the κ of the roughened SiNW is 70% lower than that of the smooth SiNW at room temperature. τ_{U}^{-1}, τ_{B}^{-1}, and τ_{I}^{-1} of phonons in these two SiNWs almost have no difference, but $\tau_{\mathrm{Bond}}^{-1}$ of the roughened SiNW is much higher than that of the smooth SiNW duo to the larger SVR of the roughened SiNW. Therefore this remarkable suppression of thermal conductivity definitely results from the mechanism of phonon–surface bond order imperfection scattering.

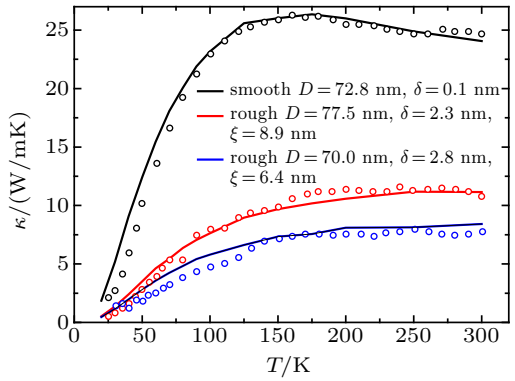

Fig. 2. Thermal conductivity of smooth and roughened SiNWs at different temperature. The solid lines present our calculations. The symbols represent experimental measurements from Ref. [40].

From Eq. (6), due to ω^4 one can expect that there is a frequency range over which phonons experience much stronger scattering from the bond order imperfections. At room temperature, τ_{U}^{-1}, τ_{B}^{-1}, τ_{I}^{-1}, and $\tau_{\mathrm{Bond}}^{-1}$ of TA phonons in smooth SiNW and roughened SiNW as a function of ω are displayed in Figs. 3(a) and 3(b), respectively. For the smooth SiNW, the phonon surface scattering due to the bond order imperfections dominates over Umklapp scattering and classical boundary scattering when ω is larger than 24 Trad/s. This threshold value ω_{c} shifts to 17 Trad/s for the roughened SiNW. According to the quadratic approximation dispersion and the Bose–Einstein distribution, there are about 72% (90%) TA phonons whose angular frequency is larger than 24 Trad/s (17 Trad/s) at room temperature. Obviously, in the roughened SiNW there are more phonons suffering severe scattering by the surface

bond order imperfections, therefore the thermal conductivity of the roughened SiNW is much lower than that of the smooth SiNW. The strongly frequency-dependent phonon–surface bond order imperfection scattering mechanism indicates that it is possible to filter high-frequency phonons and increase the contribution of low-frequency phonons, provide new pathways for manipulating phonons and controlling heat flows by surface engineering, which has been verified by the experimentally measured ballistic phonon transport at room temperature in holey silicon.[42] At low temperature, the low-frequency phonons are the majority according to the Bose–Einstein distribution. Since the phonon–surface bond order imperfection scattering has little impact on low energy phonons, low temperature discrepancy in Fig. 2 might originate from the isotropic dispersions rather than the full ones.

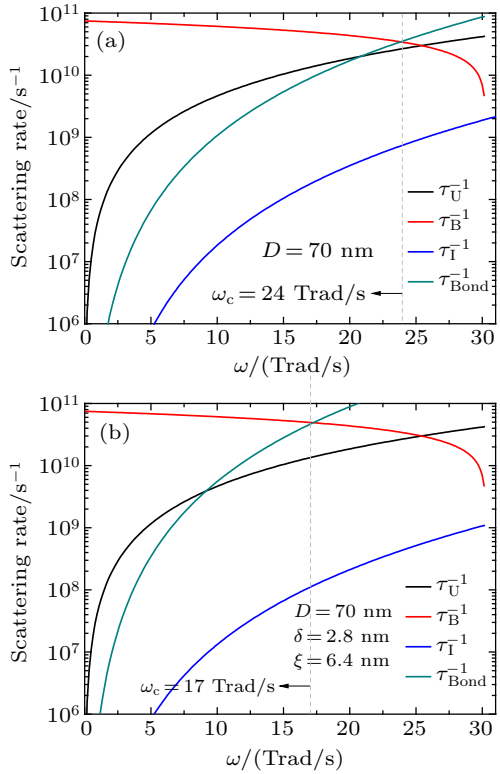

Fig. 3. Phonon scattering rates in smooth SiNW (a) and roughened SiNW (b) as functions of phonon angular frequency.

Figure 4 shows the contour plots of thermal conductivities of 70-nm-diameter SiNWs as a function of ξ and δ for the exponential and Gaussian correlations, respectively. Meeting the expectations, κ decreases with decreasing ξ and increasing δ. The effect of parameter δ on the thermal conductivity is much stronger than that of ξ. These results are consistent with phonon Monte Carlo simulations[54] and experimental measurements.[40]

Additionally, as demonstrated in Fig. 4, in the case of the same parameters D, δ, and ξ, κ of SiNWs with exponential surface is lower than that with Gaussian surface. Because the roughness surface profiles are generated from the inverse Fourier transform of power spectrum density $S(q)$ in Eq. (11), we compare $S(q)$ of exponential surface and Gaussian surface in Fig. 5(a). It is evident that for large spatial frequency of roughness, $S(q)$ of exponential surface is much higher than that of Gaussian surface. From the inverse Fourier transform in Eq. (11), it is expected that the high-frequency roughness is generated from the $S(q)$ with large spatial frequency of roughness q, therefore the exponential surface has more high-frequency roughness than the Gaussian surface, which is clearly shown in Fig. 5(b). The high-frequency and small-scale roughness results in larger SVR of exponential surface than that of Gaussian surface, which indicates that phonons are scattered more frequently by exponential surface than Gaussian surface according to Eq. (6). Therefore with the same parameters D, δ, and ξ, the suppression of exponential rough surface on thermal conductivity is stronger than that of Gaussian surface. Our phonon surface scattering mechanism is a good interpret of the experimental work in Ref. [40], which first provided the evidence for frequency-dependent phonon scattering from roughened surfaces.

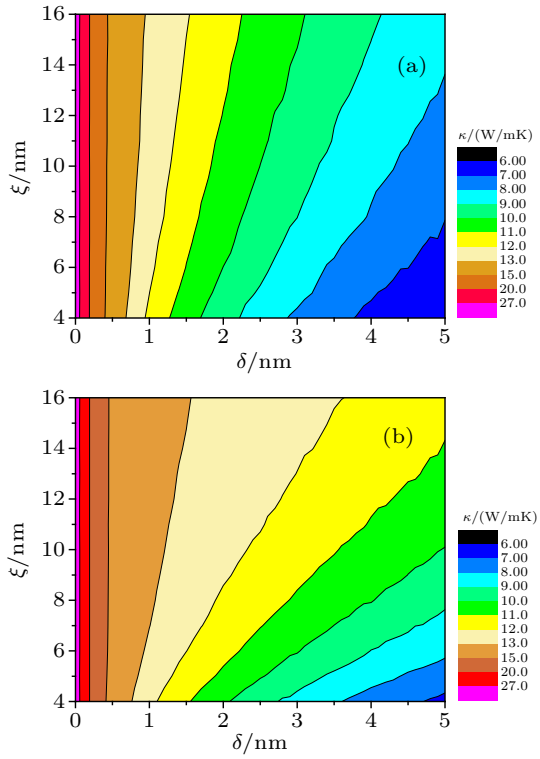

Fig. 4. Contour plots of thermal conductivity as a function of δ and ξ for exponential (a) and Gaussian (b) correlation surfaces.

In order to further understand the sensitivity of the individual parameter on the κ of the roughened SiNWs with exponential or Gaussian surface, we get 50 samples according to the uniform distribution of parameters, D: 50–100 nm, δ: 1.0n–5.0n, ξ: 5.0–15.0 nm, calculate κ of the roughened SiNWs with these parameters, and plot the scatter diagram in Figs. 6(a)–6(c). It is demonstrated that the sensitivity of parameters on κ of SiNWs is quite different. D of SiNWs with

Gaussian surface is more sensitive than that with exponential surface, while δ of SiNWs with exponential rough surface is more sensitive than that with Gaussian surface. The same as the experimental measurements,[40] the sensitivity of the correlation length ξ is very poor, which indicates that ξ by itself does not capture the surface roughness accurately for both exponential surface and Gaussian surface. Although the parameters D, δ, and ξ are relevant for phonon scattering, the relationship between them and thermal conductivity is not very strong and shows scatter, as shown in Figs. 6(a)–6(c). We plot κ vs. SVR in Fig. 6(d) and find that the SVR is nearly an universal gauge for thermal conductivity of the roughened SiNWs, regardless of exponential or Gaussian surface.

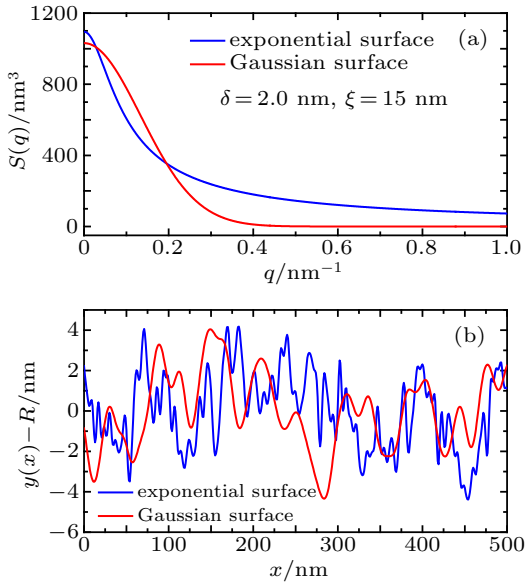

Fig. 5. (a) Power spectrum density of exponential surface and Gaussian surface. (b) Rough surface profiles generated from exponential and Gaussian ACFs.

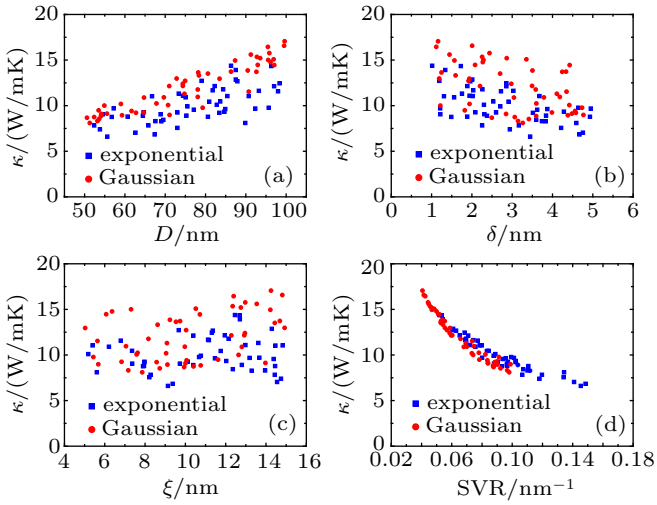

Fig. 6. Thermal conductivity as a function of parameters (a) diameter, (b) rms of roughness, (c) correlation length of roughness, and (d) surface-to-volume ratio.

In our previous work, we found that the introduction of dense hole obviously increased the surface-to-volume ratio of two-dimensional phononic crystals and remarkably suppressed the thermal conductivity due to the mechanism of phonon–surface bond order imperfection scattering.[45] Combined with this work, we make clear the underlying physical mechanism why increasing the surface-to-volume ratio of nanostructures is an effective strategy of surface engineering for blocking heat conduction.

4. Conclusion

In summary, by combining the phonon–surface bond order imperfection scattering mechanism with phonon BTE, our investigation reproduced the ultra-low κ of intentionally roughened SiNWs, and revealed that the surface bond order imperfections played the dominant role in hindering transport of high-frequency phonons, therefore resulted in the remarkable reduction of κ. Additionally, the quantitative effects of parameters D, δ, ξ, and ACF of surface on thermal conductivity of roughened SiNWs have been detailedly studied. In particular, we found that the surface-to-volume ratio was nearly an universal gauge for thermal conductivity of roughened SiNWs. This work is helpful not only to understand the blocking of surface on thermal transport in nanostructures, but also to modulate the phonon transport by surface engineering.

References

[1] Vineis C J, Shakouri A, Majumdar A and Kanatzidis M G 2010 *Adv. Mater.* **22** 3970
[2] Lee J, Lee W, Lim J, Yu Y, Kong Q, Urban J J and Yang P 2016 *Nano Lett.* **16** 4133
[3] Balandin A A 2011 *Nat. Mater.* **10** 569
[4] Zhu X L, Liu P F, Zhang J, Zhang P, Zhou W X, Xie G F and Wang B T 2019 *Nanoscale* **11** 19923
[5] Ding Z D, An M, Mo S Q, Yu X X, Jin Z L, Liao Y X, Esfarjani K, Lü J T, Shiomi J and Yang N 2019 *J. Mater. Chem. A.* **7** 2114
[6] Tang L P, Li Q Z, Zhang C X, Ning F, Zhou W X, Tang L M and Chen K Q 2019 *J. Magn. Magn. Mater.* **488** 165354
[7] Ouyang T, Jiang E, Tang C, Li J, He C and Zhong J 2018 *J. Mater. Chem. A.* **6** 21532
[8] Zeng Y J, Wu D, Cao X H, Zhou W X, Tang L M and Chen K Q 2020 *Adv. Funct. Mater.* **30** 1903873
[9] Xiao H, Cao W, Ouyang T, Xu X, Ding Y and Zhong J 2018 *Appl. Phys. Lett.* **112** 233107
[10] Wu D, Cao X H, Chen S Z, Tang L M, Feng Y X, Chen K Q and Zhou W X 2019 *J. Mater. Chem. A* **7** 19037
[11] Zhu X L, Liu P F, Xie G F, Zhou W X, Wang B T and Zhang G 2019 *Nanomaterials* **9** 597
[12] Chang C W, Okawa D, Majumdar A and Zettl A 2006 *Science* **314** 1121
[13] Cao B Y, Zou J H, Hu G J and Cao G X 2018 *Appl. Phys. Lett.* **112** 041603
[14] Yang J K, Yang Y, Waltermire S W, Wu X X, Zhang H T, Gutu T, Jiang T F, Chen Y F, Zinn A A, Prasher R, Xu T T and Li D Y 2012 *Nat. Nanotechnol.* **7** 91
[15] Chen X K, Liu J, Xie Z X, Zhang Y, Deng Y X and Chen K Q 2018 *Appl. Phys. Lett.* **113** 121906
[16] Wang H, Hu S, Takahashi K, Zhang X, Takamatsu H and Chen J 2017 *Nat. Commun.* **8** 15843
[17] Li D, Gao J, Cheng P, He J, Yin Y, Hu Y, Chen L, Cheng Y and Zhao J 2020 *Adv. Funct. Mater.* **30** 1904349
[18] Zhou W X, Chen Y, Chen K Q, Xie G F, Wang T and Zhang G 2020 *Adv. Funct. Mater.* **30** 1903829
[19] Yin Y, Li D, Hu Y, Ding G, Zhou H and Zhang G 2020 *Nanotechnology*
[20] Chen X K and Chen K Q 2020 *J. Phys.: Condens. Matter* **32** 153002

[21] Zhu X L, Liu P F, Xie G F and Wang B T 2019 *Phys. Chem. Chem. Phys.* **21** 10931
[22] Hua Y C and Cao B Y 2018 *J. Appl. Phys.* **123** 114304
[23] Xie Z X, Liu J Z, Yu X, Wang H B, Deng Y X, Li K M and Zhang Y 2015 *J. Appl. Phys.* **117** 114308
[24] Xie Z X, Zhang Y, Yu X, Li K M and Chen Q 2014 *J. Appl. Phys.* **115** 104309
[25] Xie G F, Ding D and Zhang G 2018 *Adv. Phys. X* **3** 1480417
[26] Majumdar A 1993 *J. Heat Transfer* **115** 7
[27] Nika D L, Cocemasov A I, Isacova C I, Balandin A A, Fomin V M and Schmidt O G 2012 *Phys. Rev. B.* **85** 205439
[28] Nika D L, Askerov A S and Balandin A A 2012 *Nano Lett.* **12** 3238
[29] Ziman J M 1960 *Electrons and Phonons* (Clarendon: Oxford) p. 35
[30] Dames C and Chen G 2004 *J. Appl. Phys.* **95** 682
[31] Xie G F, Guo Y, Wei X L, Zhang K W, Sun L Z, Zhong J X and Zhang Y W 2014 *Appl. Phys. Lett.* **104** 233901
[32] Aksamija Z and Knezevic I 2011 *Appl. Phys. Lett.* **98** 141919
[33] Kazan M, Guisbiers G, Pereira S, Correia M R, Masri P, Bruyant A, Volz S and Royer P 2010 *J. Appl. Phys.* **107** 083503
[34] Heron J S, Fournier T, Mingo N and Bourgeois O 2009 *Nano Lett.* **9** 1861
[35] Li D Y, Wu Y Y, Kim P, Shi L, Yang P D and Majumdar A 2003 *Appl. Phys. Lett.* **83** 2934
[36] Hochbaum A I, Chen R K, Delgado R D, Liang W J, Garnett E C, Najarian M, Majumdar A and Yang P D 2008 *Nature* **451** 163
[37] Moore A L, Saha S K, Prasher R S and Shi L 2008 *Appl. Phys. Lett.* **93** 083112
[38] Martin P, Aksamija Z, Pop E and Ravaioli U 2009 *Phys. Rev. Lett.* **102** 125503
[39] Sadhu J and Sinha S 2011 *Phys. Rev. B.* **84** 115450
[40] Lim J, Hippalgaonkar K, Andrews S C, Majumdar A and Yang P 2012 *Nano Lett.* **12** 2475
[41] Malhotra1 A and Maldovan M 2016 *Sci. Rep.* **6** 25818
[42] Lee J, Lim J and Yang P D 2015 *Nano Lett.* **15** 3273
[43] Pauling L 1947 *J. Am. Chem. Soc.* **69** 542
[44] Sun C Q 2007 *Prog. Solid State. Chem.* **35** 1
[45] Xie G F, Ju Z F, Zhou K K, Wei X L, Guo Z X, Cai Y Q and Zhang G 2018 *npj Comput. Mater.* **4** 21
[46] McGaughey A J, Landry E S, Sellan D P and Amon C H 2011 *Appl. Phys. Lett.* **99** 131904
[47] Yang F and Dames C 2013 *Phys. Rev. B.* **87** 035437
[48] Pop E, Dutton R W and Goodson K E 2004 *J. Appl. Phys.* **96** 4998
[49] Dolling G and Ekland S 1963 *In inelastic scattering of neutrons in solids and liquids* (IAEA: Vienna) p. 37
[50] Morelli D, Heremans J and Slack G 2002 *Phys. Rev. B.* **66** 195304
[51] Mingo N 2003 *Phys. Rev. B.* **68** 113308
[52] Goodnick S M, Ferry D K, Wilmsen C W, Liliental Z, Fathy D and Krivanek O L 1985 *Phys. Rev. B.* **32** 8171
[53] Buran C, Pala M G, Bescond M, Dubois M and Mouis M 2009 *IEEE Trans. Elect. Dev.* **56** 2186
[54] Maurer L Aksamija N Z, Ramayya E B, Davoody A H and Knezevic I 2015 *Appl. Phys. Lett.* **106** 133108